Force Tracking Impedance Control of Robot Manipulators Under Unknown Environment

Seul Jung, T. C. Hsia, and Robert G. Bonitz

***Abstract*—In this paper, a new simple stable force tracking impedance control scheme that has the capability to track a specified desired force and to compensate for uncertainties in environment location and stiffness as well as in robot dynamic model is proposed. The uncertainties in robot dynamics are compensated by the robust position control algorithm. After contact, in force controllable direction the new impedance function is realized based on a desired force, environment stiffness and a position error. The new impedance function is simple and stable. The force error is minimized by using an adaptive technique. Stability and convergence of the adaptive technique are analyzed for a stable force tracking execution. Simulation studies with a three link rotary robot manipulator are shown to demonstrate the robustness of the proposed scheme under uncertainties in robot dynamics, and little knowledges of environment position and environment stiffness. Experimental results are carried out to confirm the proposed controller's performance.**

***Index Terms*—Force tracking, impedance control, robust robot control, uncertainties, unknown environment.**

I. Introduction

FORCE control has been known to be one of the complicated control algorithms for robot to manipulate with other objects. Specially when the robot interacts with the environment, the desired force should be maintained while following the desired trajectories. Typical force control applications are peg in the hole operation, deburring, grinding, man–human interface, etc. Even though the demand of applying a force control technique is increasing, many problems still remain to be solved.

Impedance force control is one of the main force control algorithms in the literature with the hybrid position and force control [1]–[4]. Impedance function is realized by the relationship between force and position/velocity error. After the pioneering work of the impedance control by Hogan [5] there have been several major research issues to be solved on the impedance control. First, a position tracking error due to unknown robot dynamic uncertainty should be minimized. Second, a desired force should be directly commanded to have the force tracking capability. Third, the controller must be robust enough to deal with unknown environment stiffness and position. Those uncertainties are mainly occurred due to an inexact model of robot dynamics and the unknown environment characteristics such as unknown position and stiffness of the environment.

Within this impedance force control framework, many efforts have been made to solve these problems. Contact stability of the impedance control for stable execution of tasks has been analyzed [6], [7]. Force control has been analyzed based on a linear model [8], [9]. In addition to those efforts, various control algorithms have been proposed. Lasky and Hsia [10] have proposed the inner/outer loop control scheme where the robot dynamics uncertainties are compensated by a robust position control algorithm in the inner loop and estimated environment position is modified using an integral control of the force tracking error in the outer loop. The generalized impedance control of considering a general dynamic relation between a position error and a force error to deal with the unknown environment stiffness has been proposed [11]. The adaptive techniques of using force tracking errors have been proposed to estimate environment stiffness or adjust controller gains to compensate for unknown environment stiffness [12]–[14]. The authors have proposed a simple trajectory modification scheme using the robot controller to compensate for robot dynamics uncertainties as in [10] and environment stiffness is replaced by contact force information [15]. Later analysis has shown that accurate force tracking is not always guaranteed unless the accuracy of the estimated environment position is within certain bounds [16]. Further than that the authors have proposed an intelligent force control algorithm using a neural network to compensate for uncertainties [17]–[19]. Fuzzy-neuro techniques have been used for force control of unknown objects [20], [21]. The adaptive technique has been used to minimize the force error directly [22].

The purpose of this paper is to provide a simple solution to the force tracking impedance control algorithm that is robust with respect to uncertainties in both robot dynamic model and environment position and stiffness. The main idea is to minimize the force error directly by using a simple adaptive gain when tracking unknown environment. Environment stiffness knowledge is not required by the algorithm. The proposed control law is very simple so that it can be easily implemented in real robot control systems.

Stability and convergence of the proposed control algorithm have been analyzed. The bound of adaptive gains is found for stable force tracking execution. Simulation results confirm the theoretical stability analysis. Extensive simulation studies of a three link rotary robot manipulator are carried out to demonstrate the robustness under uncertainties in robot dynamics, environment position, and environment stiffness. Experimental results using a PUMA 560 robot arm are presented to confirm the performance of the control scheme.

Manuscript received July 11, 2002. Manuscript received in final form June 2, 2003. Recommended by Associate Editor F. Ghorbel.

S. Jung is with the Intelligent Systems and Emotional Engineering Laboratory, Chungnam National University, Daejeon 305-764, Korea (e-mail: jungs@cnu.ac.kr).

T. C. Hsia and R. G. Bonitz are with the Robotics Research Laboratory, Department of Electrical and Computer Engineering, University of California, Davis, CA 95616 USA (e-mail: hsia@ece.ucdavis.edu)

Digital Object Identifier 10.1109/TCST.2004.824320

II. Impedance Force Control

The dynamic equation of an n degrees-of-freedom manipulator in joint space coordinates are given by

$$D(q)\ddot{q} + C(q,\dot{q})\dot{q} + g(q) + \tau_f(\dot{q}) = \tau - \tau_e \tag{1}$$

where the vectors $q, \dot{q}, \ddot{q}$ are the joint angle, the joint angular velocity, and the joint angular acceleration, respectively; $D(q)$ is the $n \times n$ symmetric positive definite inertia matrix; $C(q,\dot{q})\dot{q}$ is the $n \times 1$ vector of Coriolis and centrifugal torques; $g(q)$ is the $n \times 1$ gravitational torques; τ_f is the $n \times 1$ vector of actuator joint friction forces; τ is the $n \times 1$ vector of actuator joint torques; τ_e is the $n \times 1$ vector of external disturbance joint torques.

For simplicity, let us denote $h(q,\dot{q}) = C(q,\dot{q})\dot{q} + g(q)$ so that (1) can be rewritten as

$$D(q)\ddot{q} + h(q,\dot{q}) + \tau_f(\dot{q}) = \tau - \tau_e \tag{2}$$

The corresponding Cartesian space representation is

$$D^*\ddot{X} + h^* + F_f^* = F - F_e \tag{3}$$

where $D^* = J^{T^{-1}} D J^{-1}, h^* = J^{T^{-1}} h - D^* \dot{J} J^{-1} \dot{X}$ and $F_f^* = J^{T^{-1}} \tau_f$ and J is the Jacobian matrix that must be square and invertible.

In most practical cases, the exact knowledge of D, h, τ_f are not known, thus only nominal estimates of the robot model are available for the controller design.

The basic impedance control concept is to regulate the relationship between force and position by setting suitable gains of impedance parameters. The control law F for impedance force control then is

$$F = \hat{D}^* V + \hat{h}^* + F_e \tag{4}$$

where $\hat{D}^*$and$\hat{h}^*$ are estimates of D^*, h^*, and F_e is the force exerted on the environment.

The control input V is given by

$$V = \ddot{X}_r + M^{-1}[B(\dot{X}_r - \dot{X}) + K(X_r - X) - F_e] \tag{5}$$

where M, B, and K are diagonal $n \times n$ symmetric positive definite matrices of desired inertia, damping, and stiffness gains, respectively, and X_r is the reference end-point trajectory determined from environment position, environment stiffness and desired contact force.

Combining (3)–(5) yields the closed-loop tracking error equation

$$\ddot{E} + M^{-1}[B\dot{E} + KE - F_e] = \hat{D}^{*^{-1}}[\Delta D^* \ddot{x} + \Delta h^* + F_f^*] \tag{6}$$

where $\Delta D^* = D^* - \hat{D}^*, \Delta h = h^* - \hat{h}^*$, and $E = (X_r - X)$. In the ideal case where $\Delta D^* = \Delta h^* = 0$, and $F_f^* = 0$, and the reference trajectory X_r is known exactly, the closed-loop robot satisfies the target impedance relationship

$$F_e = M\ddot{E} + B\dot{E} + KE \tag{7}$$

where F_e is equal to the desired force F_d. Since there are always uncertainties in the robot dynamic model the ideal target impedance relationships (7) can not be achieved in general. Thus, the impedance based force control is not robust in practice.

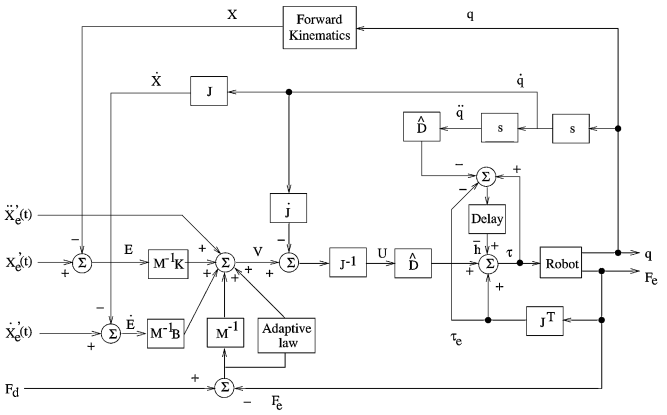

Fig. 1. Force control structure with robust position control algorithm.

Another problem is the difficulty of knowing the environment stiffness accurately in advance for us to design the reference trajectory X_r to achieve the desired contact force. These difficulties can be solved by the force tracking impedance control in the next section.

III. Force Tracking Impedance Control Scheme

The proposed control structure is shown in Fig. 1. Replacing X_r with X_e in (7) and subtracting the desired force F_d from F_e yields the new impedance function

$$F_e - F_d = M\ddot{E} + B\dot{E} + KE \tag{8}$$

where $E = X_e - X$ when $X_r = X_e$ and X_e is the environment position.

For simplicity, we consider that force is applied to only one direction. Let f_d, f_e, m, b, k be elements of F_d, F_e, M, B, K respectively. Then, (8) becomes

$$m\ddot{e} + b\dot{e} + ke - f_e + f_d = 0 \tag{9}$$

where $e = x_e - x$.

We propose a two-phase control algorithm: the first phase is free-space control when the robot is approaching toward the environment and the second phase is contact-space control in which the end-effector is in contact with the environment. In free space control, the control law can be obtained from (9) for $f_e = 0$ as follows:

$$m\ddot{e} + b\dot{e} + ke = -f_d. \tag{10}$$

We note that if the desired force f_d is set to zero in the (10) when the environment position is known exactly, then the robot would just make contact with the environment. The desired force f_d in (10) serves as the driving force to enable the robot to exert a force on the environment.

In contact space, careful investigation of the impedance relation (9) suggests that setting the stiffness gain k to zero will satisfy the ideal steady state condition in $f_e = f_d$ for any k_e. So

the proposed law is to set the stiffness gain $k = 0$ in the force controllable direction at the time of contact, that is (9) becomes

$$m\ddot{e} + b\dot{e} - f_e + f_d = 0. \tag{11}$$

However, the stiffness gain k will not be changed in the position controllable direction. Substituting $f_e = k_e(x - x_e) = -k_e e$ in (11) yields the contact space impedance law

$$m\ddot{e} + b\dot{e} + k_e e = -f_d. \tag{12}$$

We see that (12) is asymptotically stable. Even though k_e is not known exactly in practice, the proper gains m and b based on approximation of k_e can be chosen to assume a good transient response of (11). Therefore, our proposed impedance function is simple, stable and robust in force tracking under unknown environment stiffness condition.

IV. Adaptive Impedance Force Control

Consider for the practical case that we have an inaccurate environment position estimate x_e' and $\delta x_e = x_e' - x_e$ which is the uncertainty of x_e. Define $e' = e + \delta x_e$, then e' will replace e in both (10) and (12) yielding

$$m\ddot{e}' + b\dot{e}' + ke' = -f_d \text{ (free space)} \tag{13}$$

$$m\ddot{e}' + b\dot{e}' = f_e - f_d \text{ (contact space)} \tag{14}$$

where δx_e is the inaccuracy of the environment position which can be specified by the control designer. For free space motion (13), our previous analysis has shown that when $\delta x_e < 0$ the robot manipulator may not always make contact with the environment [16]. On the other hand, the contact can always be made when $\delta x_e > 0$. Therefore, we should always overestimate the environment position x_e' such that $\delta x_e > 0$ to guarantee contact will always occur.

For contact space (14), we can easily show that the exact force tracking can be achieved if the environment is a flat surface where x_e is a constant and x_e' is also a constant satisfying $x_e' - x_e > 0$. In this case, (14) becomes

$$m\ddot{x} + b\dot{x} = f_d - f_e. \tag{15}$$

Hence, $f_e = f_d$ in a steady state. However when f_d, x_e, and δx_e are time varying, a force tracking error will occur. For example, there will be a finite steady state force tracking error when f_d and/or δx_e are ramp functions, and the force error would become infinite if f_d and/or δx_e are parabolic functions.

So, we propose the new adaptive impedance equation as

$$m\ddot{e}' + b(\dot{e}' + \Omega) = f_e - f_d \text{ (contact space)}. \tag{16}$$

Here, Ω is adjusted online according to the force error. The proposed simple adaptive law of compensating for $m\ddot{x}_e' + b\dot{x}_e'$ is

$$\Omega(t) = \Omega(t - \lambda) + \eta\frac{(f_d(t - \lambda) - f_e(t - \lambda))}{b} \quad \eta > 0 \tag{17}$$

where η is the update rate and λ is the sampling period of the controller.

In the following section, we will show that the impedance control algorithm (16) with (17) is stable and the force tracking error is zero.

V. Stability and Convergence of Adaptive Control Law

When the adaptive law (17) is employed in the control loop (16), it is necessary to see whether the new control law remains stable. Combining (16) and (17) yields

$$m\ddot{e}(t)' + b\dot{e}(t)' + k_e e(t) + b\Omega(t - \lambda) + \eta k_e e(t - \lambda) = -(f_d(t) + \eta f_d(t - \lambda)). \tag{18}$$

From the relationship $f_e = k_e(x - x_e)$, we can express

$$x = x_e + \frac{f_e}{k_e} \quad \dot{x} = \dot{x}_e + \frac{\dot{f}_e}{k_e} \quad \ddot{x} = \ddot{x}_e + \frac{\ddot{f}_e}{k_e}. \tag{19}$$

Substituting $x, \dot{x}, \ddot{x}$ into (19) yields the second-order force error equation as

$$\begin{aligned} m(\ddot{f}_d - \ddot{f}_e) + b(\dot{f}_d - \dot{f}_e) + b\Omega(t - \lambda) + k_e(f_d - f_e) \\ = m\ddot{f}_d + b\dot{f}_d - mk_e\delta\ddot{x}_e - bk_e\delta\dot{x}_e \\ - \eta k_e(f_d(t - \lambda) - f_e(t - \lambda)). \end{aligned} \tag{20}$$

Defining $\epsilon(t) = f_d(t) - f_e(t)$ and rewrite (20) as

$$\begin{aligned} m\ddot{\epsilon}(t) + b\dot{\epsilon}(t) + k_e(\epsilon(t) + b\Omega(t - \lambda) + \eta\epsilon(t - \lambda)) \\ = m\ddot{f}_d + b\dot{f}_d - mk_e\delta\ddot{x}_e - bk_e\delta\dot{x}_e. \end{aligned} \tag{21}$$

Consider k elements of Ω series

$$\begin{aligned} b\Omega(t - \lambda) = b\Omega(t - (k - 1)\lambda) + \eta\epsilon(t - (k - 2)\lambda) \\ + \ldots + \eta\epsilon(t - 2\lambda). \end{aligned} \tag{22}$$

We assume that the initial Ω is zero such that $\Omega(t - (k - 1)\lambda) = 0$. Combining (21) with (22) yields

$$\begin{aligned} m\ddot{\epsilon} + b\dot{\epsilon} + k_e\epsilon + \eta k_e(\epsilon(t - (k - 1)\lambda) + \cdots + \epsilon(t - \lambda) \\ = m\ddot{f}_d + b\dot{f}_d - m\delta\ddot{x}_e - b\delta\dot{x}_e. \end{aligned} \tag{23}$$

Define the force occurred due to the estimation of the environment position as $\bar{f}_e = k_e\delta x_e$. Then, (23) becomes

$$\begin{aligned} m\ddot{\epsilon} + b\dot{\epsilon} + k_e\epsilon + \eta k_e(\epsilon(t - (k - 1)\lambda) + \cdots + \epsilon(t - \lambda) \\ = m\ddot{\varepsilon} + b\dot{\varepsilon} \end{aligned} \tag{24}$$

where $\varepsilon = f_d - \bar{f}_e$.

Laplace transform of (24) is

$$\frac{\epsilon(s)}{\mathcal{E}(s)} = \frac{ms^2 + bs}{(ms^2 + bs + k_e + k_e\eta(e^{-(k-1)\lambda s} + \cdots + e^{-\lambda s}))}. \tag{25}$$

When there is a delay λ, the stability of the system (25) can be assured by the characteristic equation of (25)

$$(ms^2 + bs + k_e + k_e\eta(e^{-(k-1)\lambda s} + \ldots + e^{-\lambda s})) = 0. \tag{26}$$

If $|e^{-\lambda s}| \neq 1$ where $0 < \lambda < 1$ and k is assumed to be a large number, the sum of the series can be represented as

$$\sum_{n=1}^{\infty} e^{-\lambda s n} = \frac{1}{1 - e^{-\lambda s}} - 1. \tag{27}$$

Substituting the sum (27) into (26) yields

$$\left(ms^2 + bs + k_e + k_e \eta \left(\frac{e^{-\lambda s}}{1 - e^{-\lambda s}} \right) \right) \epsilon(s) = 0. \tag{28}$$

When the sampling is fast where $\lambda << 1$, the delayed term can be approximated as $e^{-\lambda s} \approx 1 - \lambda s$ by Taylor series expansion. Rearranging (28) with Taylor series expansion yields

$$\lambda m s^3 + b\lambda s^2 + k_e \lambda (1 - \eta) s + k_e \eta = 0. \tag{29}$$

For stability, the Routh–Hurwitz array is constructed

$$\begin{array}{ccc} s^3 & \lambda m & k_e \lambda (1 - \eta) \\ s^2 & b\lambda & \eta k_e \\ s^1 & c_1 & 0 \\ s^0 & c_0 & 0 \end{array} \tag{30}$$

and the following conditions are found:

$$c_1 = \frac{b k_e \lambda^2 (1 - \eta) - \lambda \eta m k_e}{b\lambda} > 0 \text{ and } c_0 = \eta k_e > 0 \tag{31}$$

since $m, b, \lambda > 0$.

In order for the (31) to be satisfied with the stability condition, η should be bounded by

$$0 < \eta < \frac{b\lambda}{b\lambda + m}. \tag{32}$$

For convergence, we investigate the steady-state error $E_{ss}(s)$ of (25)

$$E_{ss}(s) = \lim_{s \to 0} s(\epsilon(s) - \mathcal{E}(s)) = -1 \tag{33}$$

when the input is a step function such that $\mathcal{E}(s) = (1/s)$. This means that when the input $\mathcal{E}$ is a step function the output $\epsilon(s)$ goes to zero so that

$$\lim_{t \to \infty} \epsilon(t) = 0. \tag{34}$$

Therefore, when $t \to \infty$, $f_e \to f_d$. The actual force converges to the desired force.

VI. Robust Position Control Algorithm

The basic idea of the robust position control algorithm is to use the previous informations to cancel the highly complex uncertainties [23]. We can write the robot dynamic (2) as

$$\hat{D}\ddot{q}(t) + \bar{h}(t) = \tau(t) \tag{35}$$

where $\bar{h} = h(t) + \tau_f(t) + \tau_e(t) + (D - \hat{D})\ddot{q}(t)$ and $\hat{D}$ is the estimate of D.

Select the control law as

$$\tau(t) = \hat{D}u(t) + \bar{h}(t). \tag{36}$$

From the (36), $\bar{h}(t)$ can be rewritten as

$$\bar{h}(t) = \tau(t) - \hat{D}(q)\ddot{q}(t). \tag{37}$$

This idea cannot be exactly implemented in practice, however since the values for $\tau(t)$ and $\ddot{q}(t)$ are not available at the time t. It is suggested to use the delayed sample values $\tau(t - \lambda)$ and $\ddot{q}(t - \lambda)$. The new estimation of $\bar{h}(t)$, $\hat{\bar{h}}(t)$ is defined as follows:

$$\hat{\bar{h}}(t) = \bar{h}(t - \lambda) = \tau(t - \lambda) - \hat{D}(q)\ddot{q}(t - \lambda). \tag{38}$$

The delayed samples $\tau(t - \lambda)$ and $\ddot{q}(t - \lambda)$ can be easily stored at each sampling period.

Now, the control law becomes

$$\tau(t) = \hat{D}u(t) + \hat{\bar{h}}(t) \tag{39}$$

and

$$u(t) \cong \ddot{q}(t) = J^{-1}(V - \dot{J}\dot{q}) \tag{40}$$

where $V = \ddot{X}$ and J is the Jacobian matrix.

From the impedance law (16), $\ddot{X}$ can be obtained as

$$V = \begin{cases} \ddot{X}_e' + M^{-1}(F_d + B\dot{E}' + KE'), & \text{Position} \\ \ddot{X}_e' + M^{-1}(F_d - F_e + B(\dot{E}' + \Omega)), & \text{Force} \end{cases} \tag{41}$$

The control law becomes

$$\tau(t) = \hat{D}J^{-1}[V - \dot{J}\dot{q}] + \tau(t - \lambda) - \hat{D}\ddot{q}(t - \lambda). \tag{42}$$

For stability analysis of the robust position control algorithm, let us define the control input error ε caused from time sample delay from (37) and (39) as follows:

$$\varepsilon = \ddot{q} - u = \hat{D}^{-1}(\hat{\bar{h}}(t) - \bar{h}(t)) \tag{43}$$

where $\hat{\bar{h}}(t) = h(t - \lambda)$. From (39), (40), (41), and (43) the control input error ε at contact space has the following relationship with the closed-loop equation:

$$M\ddot{E}' + B\dot{E}' + K_e E = -MJ\varepsilon - F_d. \tag{44}$$

Since M, B, and K_e are positive definite the forced error system the left hand side of (44) is asymptotically stable with the result shown in an earlier section. Only a concern for the stability is the boundness of $-M\ J\varepsilon$ since the F_d is bounded. Since MJ is bounded, BIBO stability can be achieved if the error ε is bounded. The boundness of ε can be shown in the same manner of the stability proof shown in [23].

Using (38) and (43), we have

$$\begin{aligned} D(t)\varepsilon(t) &= \hat{D}u(t) + (D(t - \lambda) - \hat{D})\ddot{q}(t - \lambda) \\ &\quad + C(t - \lambda) + G(t - \lambda) + \tau_e(t - \lambda) \\ &\quad - C(t) - G(t) - \tau_e(t) \\ &= (\hat{D} - D(t))u(t) + (D(t - \lambda) - \hat{D})\ddot{q}(t - \lambda) \\ &\quad - \Delta(t) \end{aligned} \tag{45}$$

where $\Delta(t) = C(t) - C(t - \lambda) + G(t) - G(t - \lambda) + \tau_e(t) - \tau_e(t - \lambda)$.

Substituting $\ddot{q}(t - \lambda) = \varepsilon(t - \lambda) + u(t - \lambda)$ into (45) yields

$$\begin{aligned} D(t)\varepsilon(t) &= \hat{D}(u(t) - u(t - \lambda)) \\ &\quad - Du(t) + D(t - \lambda)(\varepsilon(t - \lambda) + u(t - \lambda)) \\ &\quad - \hat{D}\varepsilon(t - \lambda) - \Delta(t) \\ &= D^{-1}(t)\hat{D}(u(t) - u(t - \lambda)) \\ &\quad + D^{-1}(t)D(t - \lambda)\ddot{q}(t - \lambda) - \Delta(t) \\ &\quad + \varepsilon(t - \lambda) - D^{-1}(t)\hat{D}\varepsilon(t - \lambda) \\ &\quad - \varepsilon(t - \lambda) - u(t) + u(t - \lambda) - u(t - \lambda). \end{aligned} \tag{46}$$

Rearranging (46) yields

$$\begin{aligned}\varepsilon(t) &= [I - D^{-1}(t)\hat{D}]\varepsilon(t-\lambda) \\ &\quad - [I - D^{-1}(t)\hat{D}](u(t) - u(t-\lambda)) \\ &\quad + D^{-1}(t)[D(t-\lambda) - D(t)]\ddot{q}(t-\lambda) - \Delta(t). \quad (47)\end{aligned}$$

In discrete-time domain, it can be represented as

$$\begin{aligned}\varepsilon(k) &= [I - D^{-1}(k)\hat{D}]\varepsilon(k-1) \\ &\quad - [I - D^{-1}(k)\hat{D}](u(k) - u(k-1)) \\ &\quad + D^{-1}(k)[D(k-1) - D(k)]\ddot{q}(k-1) - \Delta(k) \\ &= [I - D^{-1}(k)\hat{D}]\varepsilon(k-1) + R(k) \quad (48)\end{aligned}$$

where $R(k) = -[I - D^{-1}(k)\hat{D}](u(k) - u(k-1)) + D^{-1}(k)[D(k-1) - D(k)]\ddot{q}(k-1) - \Delta(k)$ which is considered as a forcing function. Obviously, (48) is the first-order discrete equation and asymptotically stable if roots of $[I - D^{-1}(k)\hat{D}]$ reside inside a unit circle. Appropriate values for $\hat{D}$ should be selected to satisfy the stability [23].

It has been demonstrated in these studies that controller design approach such as (48) works quite well for the PUMA robot manipulator. With the aid of DSP hardware, λ can be made significantly small in practice. For example, our experiments with PUMA 560 arm have achieved a sampling rate of 200 Hz. Consequently, the control system is stable and the performance is very close to that of the ideal case. Further information regarding practical controller implementation can be found in [24], [25].

VII. Simulation Studies

A. Flat Wall Tracking

In this section, the proposed control algorithm is tested by simulating the tracking performance with a three link rotary robot manipulator whose parameters are taken from the first three links of PUMA 560 arm. The nominal system parameters are used as the basis in forming the robot model $\hat{D}(q)$ and $\hat{H}(q, \dot{q})$. Model uncertainties included a 10 Kg mechanical tool attached to the third link, Coulomb friction and viscous friction forces $\tau_f(\dot{q})$ added to each joint where $\tau_f(\dot{q}) = 5.0\text{sgn}(\dot{q}) + 8.0\dot{q}$.

The performances of the proposed schemes are tested by tracking a flat wall. The controller gains are selected as $M = I, B = \text{diag}[500, 40, 500]$, and $K = \text{diag}[300\,100\,300]$ which give over-damped motions at the three joints. At contact, K becomes $K = \text{diag}[0\,100\,100]$ such that the gain in force controllable direction, in this case the x axis, is set to zero. In order to test the robustness of the proposed control law to unknown environment stiffness, abruptly changing environment stiffnesses are given as

$$k_e = \begin{cases} 40000\,(\text{N/m}), & 0 \le t < 2 \\ 80000\,(\text{N/m}), & 2 \le t < 4 \\ 40000\,(\text{N/m}), & 4 \le t < 6 \end{cases} \quad (49)$$

which is considered as a stiff and flat environment. Fig. 2 shows the effect of robot dynamic uncertainties on force tracking. Force overshoots are observed due to sudden changes of environment stiffness. The resulting compensated force tracking by robust position control algorithm is excellent compared with uncompensated force.

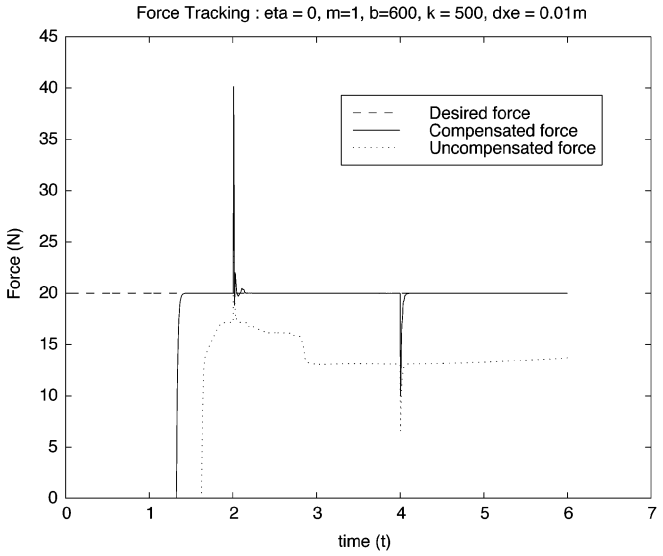

Fig. 2. Dynamic uncertainty effects on force tracking.

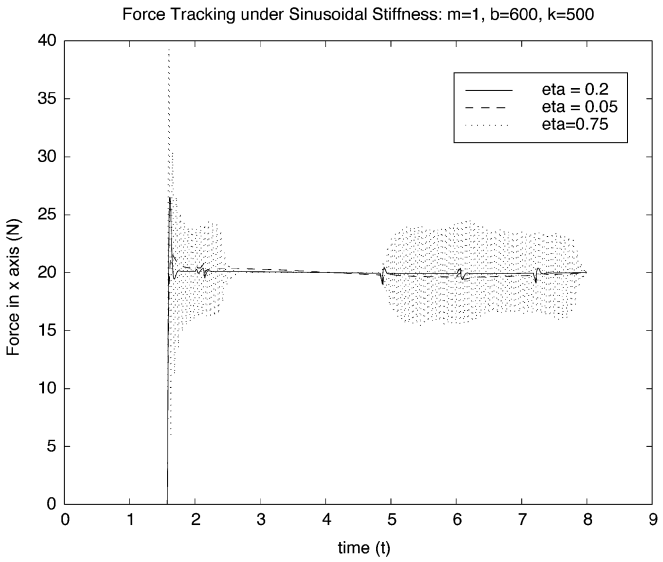

Fig. 3. Force tracking with different adaptive rates.

B. Sinusoidal Shape Wall Tracking

Another simulation is carried out for the sinusoidally shaped environment as shown in Fig. 3. Variation of environment position is 2 cm. Environment position is not known to a robot, but a robot knows the inside estimated position of the environment. The environment has the time varying continuous stiffness as follows:

$$k_e = 40\,000 + 5000\sin\left(\frac{\pi * t}{2}\right)\ (\text{N/m}). \quad (50)$$

Note that since the actual environment position x_e is not known to us in most practical case, we assume that environment position is flat. In this task, the environment stiffness is sinusoidally varying as well. We adopt the adaptive idea (17) to estimate $\dot{x}_e$ which is a major contribution term to the force deviation. Fig. 3 shows the force tracking plots using the different adaptive laws. The controller gains $B = \text{diag}[600, 20, 20], K = \text{diag}[500\,100\,100]$

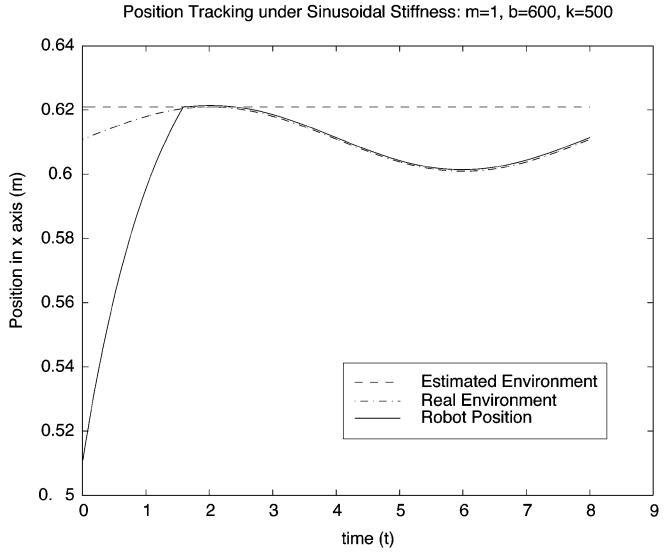

Fig. 4. Position tracking on x axis when $\eta = 0.05$.

are used in free space and $K = \mathrm{diag}[0\,100\,100]$ is used in contact space. First, the update rate is selected as $\eta = 0.75 = (600 * 0.005)/(600 * 0.005 + 1)$ which is the upper bound condition of η. The performance of force tracking is quite oscillatory as expected. Second, the update rate η is set to $0.2 < 0.75$. The force tracking performance is excellent. For a force tracking plot with $\eta = 0.05$ we notice that the initial impact force overshoot is notably minimized. However, the force error is little bit larger than that of $\eta = 0.2$. Position tracking is shown in Fig. 4. We do not observe any force overshoots due to changes of environment stiffness. The best performance can be achieved when $\eta = 0.2$. Therefore, in order to obtain the best force tracking the adaptive rate should be optimized within the stability bound.

C. Tracking Flat Wall With Triangular Crack

In this section, we test the force tracking of a flat wall with a triangular crack as shown in Fig. 5. In order to show the robustness to unknown environment stiffness of the proposed scheme, we tested the system performance for abruptly changing environment stiffnesses with the stiffness profile as

$$k_e = \begin{cases} 40000\ (\mathrm{N/m}), & 0 \le t < 3 \\ 80000\ (\mathrm{N/m}), & 3 \le t < 6 \end{cases} \tag{51}$$

which is considered as a stiff environment. In this task, we test the different values of an inaccurate estimation of an environment position such as $\delta x_e = 0.03, 0.06$, and 0.1 m. The resulting force trackings are excellent as shown in Fig. 6. We note that the larger estimation of δx_e yields the shorter contact time but the larger force overshoot at initial contact. Another task is tested for the robot to follow the flat wall with a large triangle shaped crack in the middle. The initial controller gains are selected as $M = I, B = \mathrm{diag}[440, 40, 440]$, and $K = \mathrm{diag}[300\,100\,300]$. The environment position is not correctly estimated but specified inside the environment to guarantee the contact. Since the deepest point of the crack is 0.02 m from the surface the user specified δx_e is selected at 0.03 m such that the estimated environment position $x_e' = x_e + 0.03$ m. Since

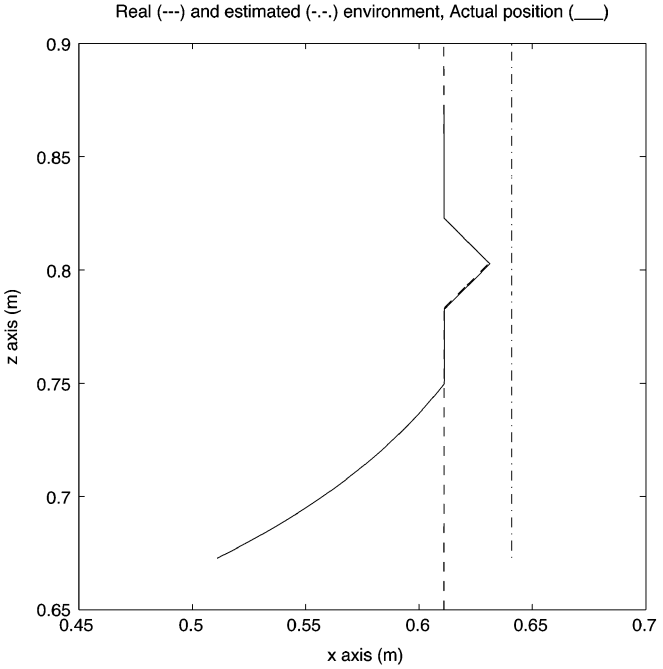

Fig. 5. Position tracking for a flat wall with a triangle crack with the adaptive law.

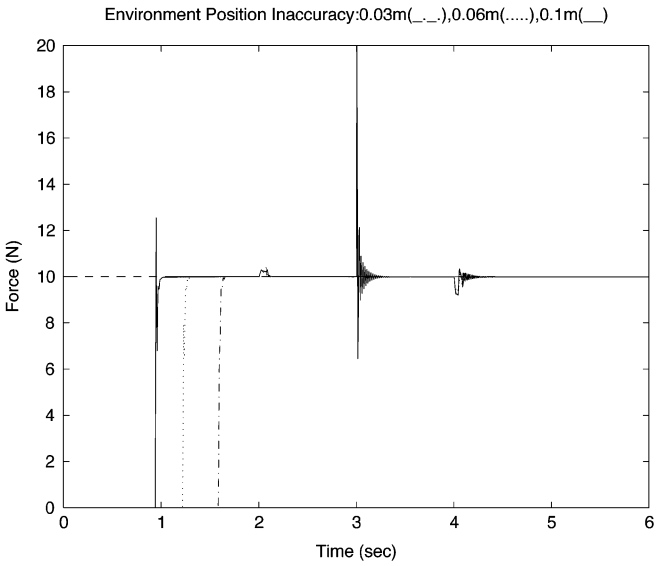

Fig. 6. Force tracking with different environment position inaccuracies δx_e.

we assume that the environment profile is not available, δx_e is constant and $\delta \dot{x}_e, \delta \ddot{x}_e$ are assumed to be zero. In this case, the control behavior is controlled by (17) and the plots are shown in Fig. 7. Even though the force tracking is excellent when the environment is flat, the force tracking is not effective with notable errors when the robot follows the crack position.

The deviation in force tracking in Fig. 7 results from not specifying $\dot{x}_e$ and $\ddot{x}_e$ in the control law because it is assumed to be unknown. The approximate value of force deviation can be calculated from $\delta f = f_d - f_e \approx b * \dot{x}_e$ in Fig. 7 since $m * \ddot{x}_e \ll b * \dot{x}_e$. In our simulation, since $b = 440$ is used and $\dot{x}_e = 0.02$ m is assumed to be unknown the $\delta f \approx 8.8(N)$ which matches the force deviation in the plot. Therefore, it is better to specify more information on the environment. The force tracking plot using

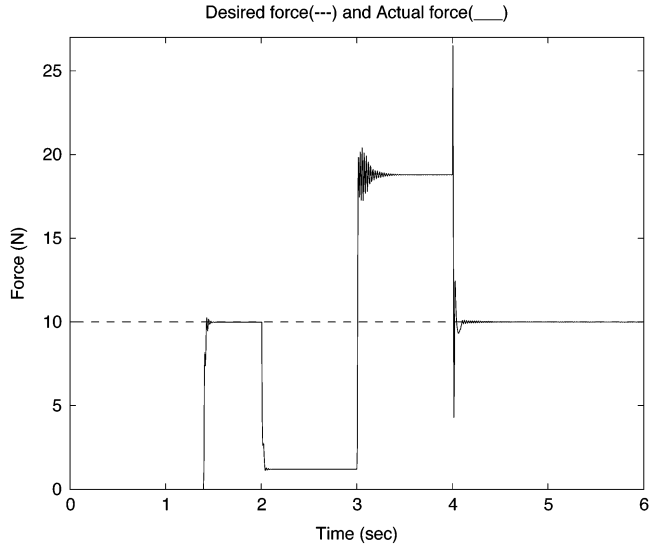

Fig. 7. Force tracking for a flat wall with a triangle crack when $\dot{x}_e = 0$.

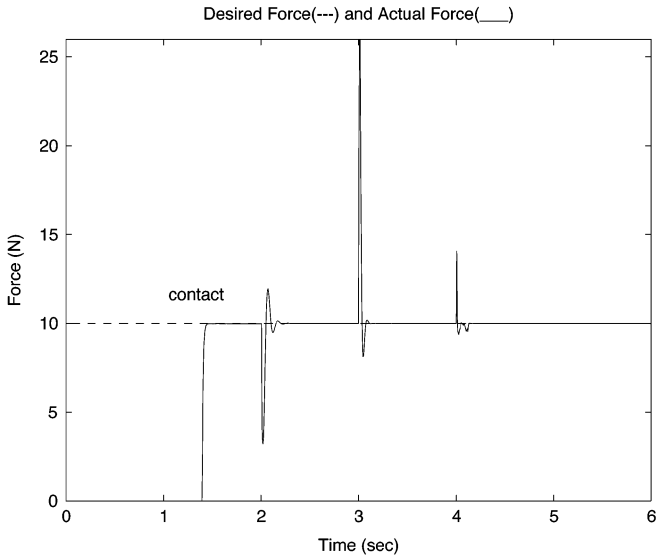

Fig. 8. Force tracking for a flat wall with a triangle crack with the adaptive law.

the adaptive law is shown in Fig. 8. The update rate is selected as $\eta = 0.3 < (440 * 0.005)/(440 * 0.005 + 1) = 0.6875$ which is satisfied the stability condition of η. The corresponding position tracking plot is shown in Fig. 5. The performance of force tracking is excellent.

D. Force Tracking on Bur

In this section, we simulated a robot deburring process. The environment with a burr on it has the time varying nonhomogeneous stiffness as follows:

$$k_e = 40000 + 5000 \sin\left(\frac{\pi * t}{2}\right) \text{ (N/m)}. \tag{52}$$

A burr is triangular shape on a flat surface as shown in Fig. 9. We assume that the exact environment(workpiece) location and stiffness are unknown. So the estimated environment location is conservatively specified further inside the environment as

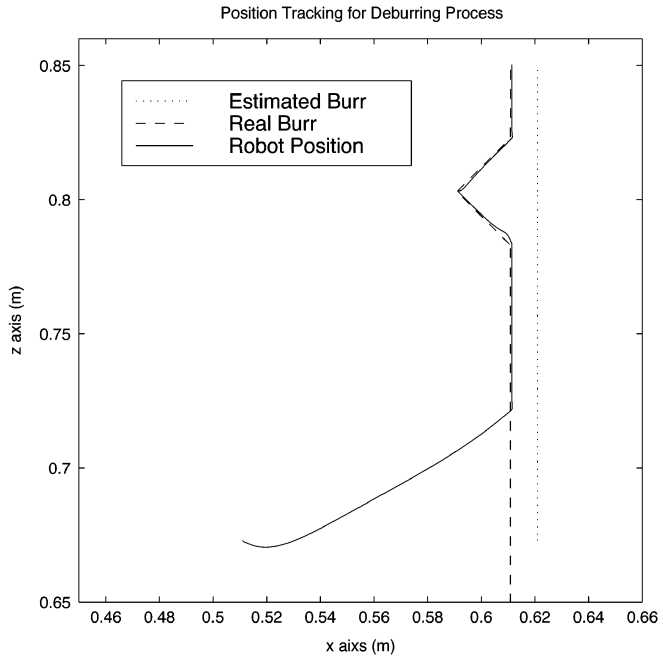

Fig. 9. Position tracking on a burr.

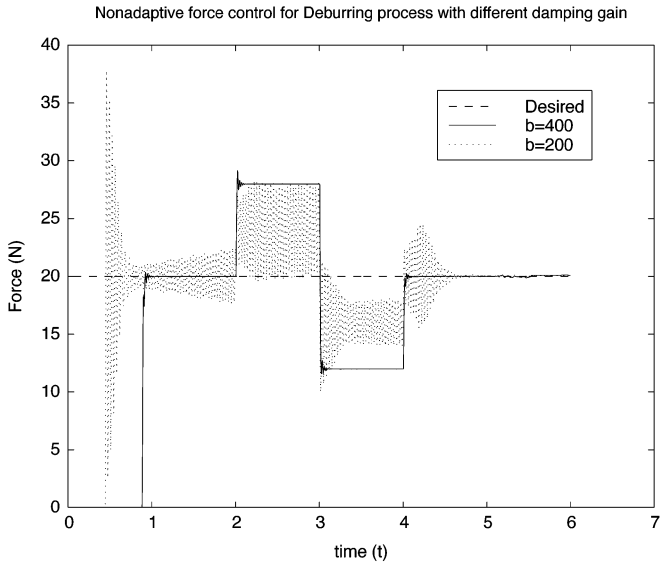

Fig. 10. Force tracking without adaptive method.

shown in Fig. 9. The environment position is specified inside the environment to guarantee the contact.

The robot is initially at rest in free space. Then it is commanded to move toward the environment and make contact.

At the first phase, the milling process is simulated. After contact, the robot is commanded to follow the trajectory in z direction with a constant force of 20 N applied to the workpiece.

At contact, the controller sets the stiffness gain in force controlled direction to zero such that $K = \text{diag}[0\,100\,100]$. Without an adaptive law compensation for uncertainties we see from Fig. 10 that commanded force tracking is not good but chattering. This is the case when the damping gain is $200 < 2 * \sqrt{40\,000} = 400$ which is a under damped case. When the damping gain is increased to 400 in order to have

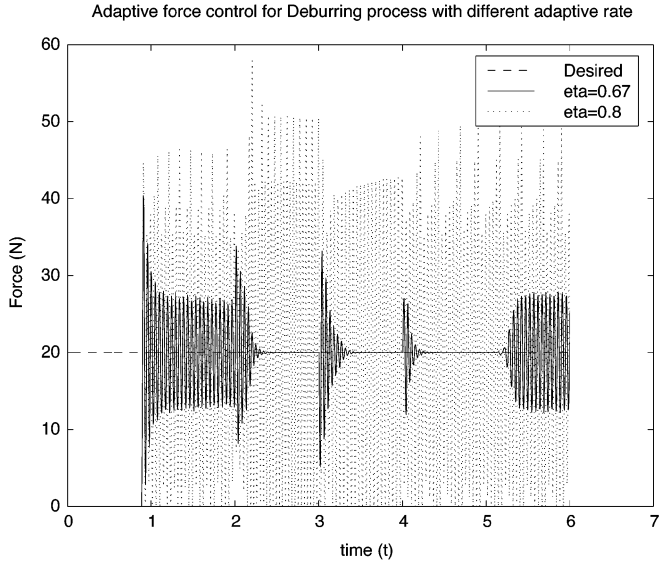

Fig. 11. Force tracking on a burr with adaptive gains outside stability bounds.

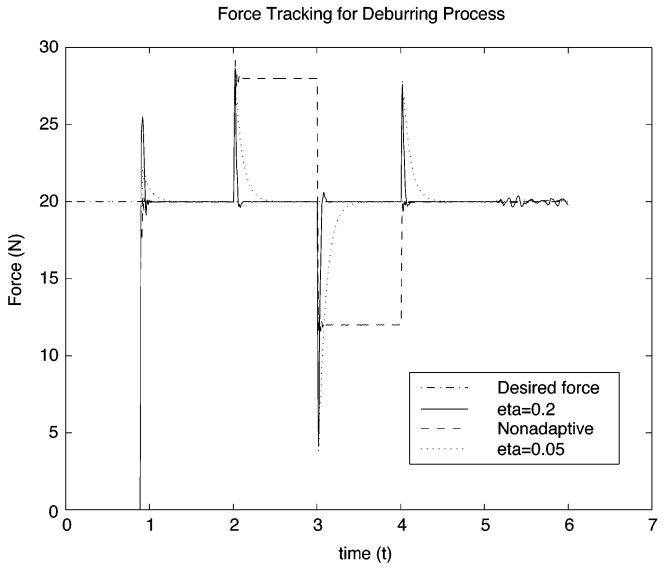

Fig. 12. Force tracking on a burr with adaptive gains inside stability bounds.

critically damped response, the oscillatory behavior is eliminated. So we select $b = \text{diag}[400\ 20\ 20]$ as damping gain. However, the large force error can be observed when the burr is detected. Then we use the adaptive technique to minimize the force error. Since we assume that the environment profile is not available, δx_e is constant and $\delta \dot{x}_e, \delta \ddot{x}_e$ are assumed to be zero. In this case, the plots are shown in Figs. 11 and 12. We test the different values of adaptive gains: $\eta = 0.67$ and 0.8 which are greater than and equal to the upper bound of stability condition in (32). The upper value of the stability bound is $\eta = (400 * 0.005)/(400 * 0.005 + 1) = 0.67$. Fig. 11 shows the resultant force tracking with an adaptive technique for different adaptive gains. The force tracking for both cases are oscillatory. When the upper bound value $\eta = 0.67$ is used, the force tracking is less oscillating. When the adaptive gain belongs to inside the stability bound the force tracking becomes better as shown in Fig. 12. Fig. 12 compares the force tracking

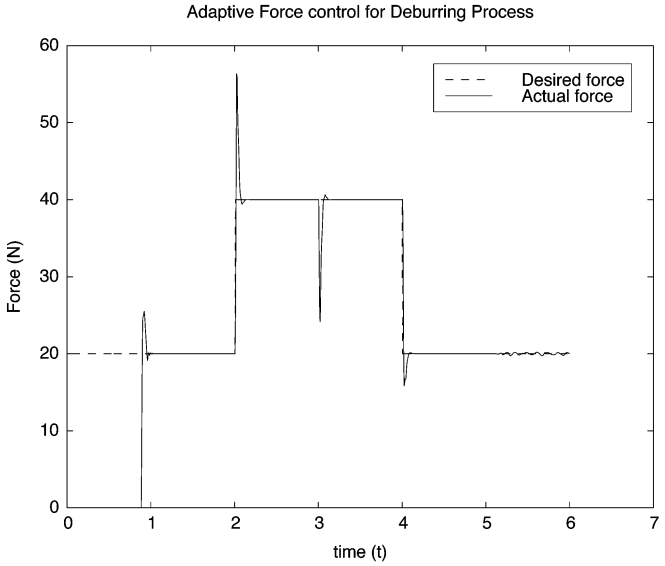

Fig. 13. Force tracking on a burr with increased force.

performances with different adaptive gains inside the bound. It clearly shows that the performance with the adaptive technique is much better than that without of the adaptive technique. We also note that the larger value of η yields the faster convergence in minimizing errors but it shows more oscillatory behavior. The best force tracking performance can be shown when $\eta = 0.2$. So the adaptive gain should be optimized within stability bounds. Another task is simulated for a deburring process in Fig. 13. The robot controller increases the desired force to 40 N to get rid of a burr when a burr is detected. Fig. 13 shows the deburring process with the increased force. It works quite well.

VIII. Experimental Studies

To demonstrate the performance of the proposed algorithm, experiments were conducted using the UCD Robotics Research Laboratory (RRL) experimental test-bed consisting of a PUMA 560 industrial manipulator fitted with a JR3 wrist force sensor. The manipulator is controlled by a UCD RRL-designed controller consisting of: 1) a 486 personal computer; 2) electronics to read the voltages from the joint potentiometers, to read each joint's digital encoder signals, and to output control signals to the Unimate motor voltage amplifiers; 3) a force sensor interface card; 4) a TMS320C40 DSP board; and 5) the control software.

Single arm experiments were first conducted on the PUMA manipulator operating in both free space and in contact with a rigid surface using conventional impedance control which resulted in the impedance chosen as follows: $M = \text{diag}\{50\ 50\ 50\ 1\ 1\ 1\}, B = \text{diag}\{3142\ 3142\ 1571\ 31.4\ 31.4\ 31.4\}$, and $K = \text{diag}\{31\,583\ 31\,583\ 11\,844\ 237\ 237\ 237\}$. The inertia matrix was chosen to satisfy a lower bound requirement which results from digital implementation during constrained operation as shown in [26]. The preceding impedance yields good trajectory tracking and force step response performance. Damping in the z direction was reduced to achieve faster response in the force tracking direction.

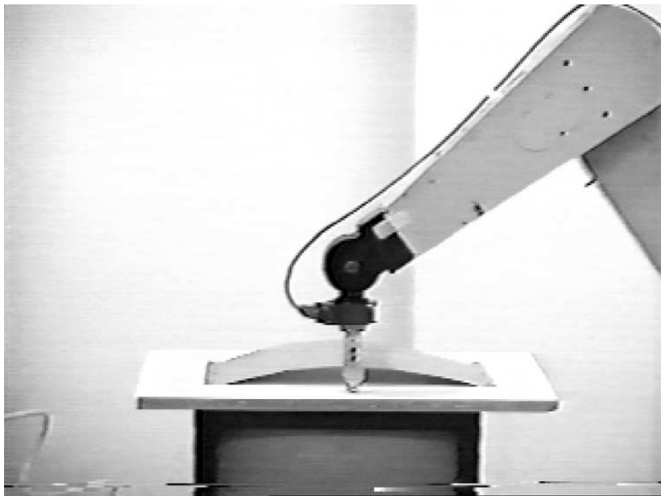

Fig. 14. Experimental setup—curved environment surface.

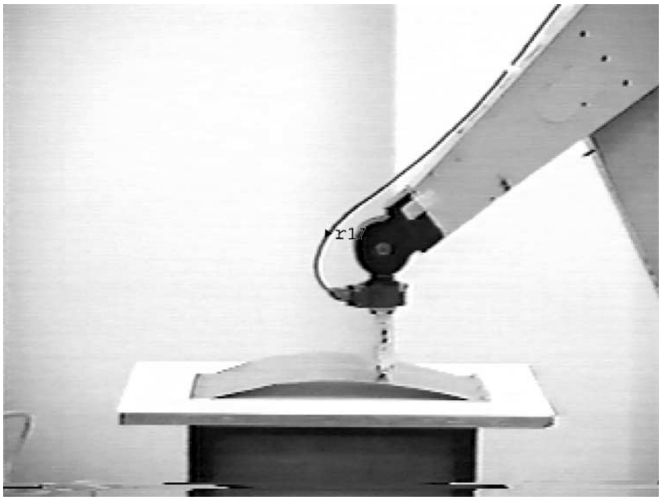

Fig. 16. Experimental setup—flat environment surface.

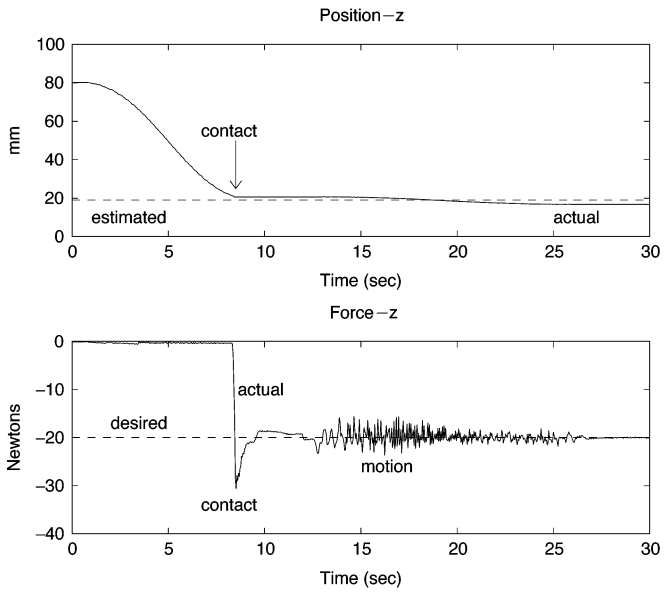

Fig. 15. Experiment—flat environment surface.

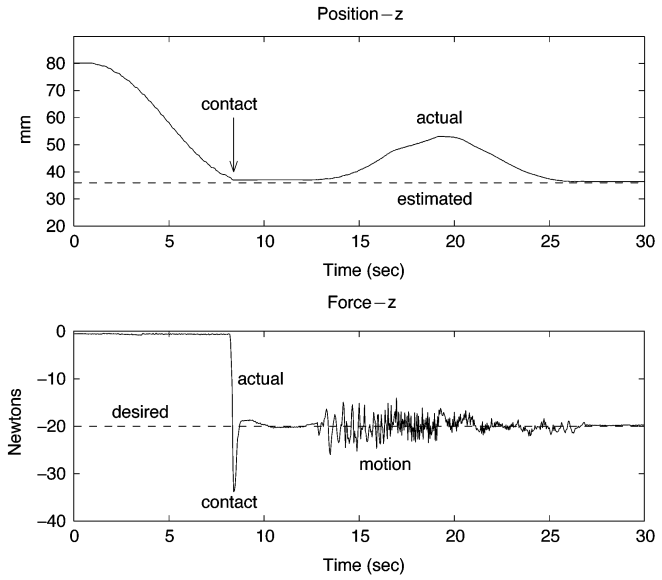

Fig. 17. Experiment—curved environment surface.

To confirm simulation studies, two experiments were conducted each consisting of moving in the negative z direction onto a surface, and then moving 25 cm along the surface in the x direction in 15 s with $f_d = [0\,0\,-20N\,0\,0\,0]$. The first surface is a flat hard surface shown in Fig. 14 and the second surface is stiff curved sheet of galvanized steel shown in Fig. 16. The exact location and stiffness of each surface is unknown. For the flat hard surface, η was chosen as 0.001 and for the curved stiff surface η was increased to 0.02 since the surface is more compliant. The results of the experiments are shown in Figs. 15 and 17. Initially, the end effector is commanded to move to a point beyond the surface. Upon contact with the surface, the initial overshoot is approximately 60% and the force settles to -20 N in approximately 2 s. During the motion the force is controlled to within $\pm 20\%$. The experiments demonstrate that the algorithm exhibits good force tracking in the presence of environmental uncertainty.

IX. Conclusion

A simple robust force control scheme of a robot manipulator is presented in this paper. The robust position control algorithm is used to compensate for the uncertainties in the robot dynamics. The new impedance controller is realized. Even though the proposed impedance function so simple, when the environment position is unknown, the estimation of a velocity profile of the environment position is necessary to achieve the better force tracking. One simple solution was suggested to use an adaptive control concept that adjusts the environment velocity profile based on a force error. Simulation results proved that the proposed controller is excellent to achieve the best force/position tracking under the situation that the environment is not known. Stable force tracking were experimentally achieved based on the analysis of convergence of adaptive gains. The proposed controller works well when the environment stiffness is abruptly changed.

REFERENCES

[1] M. H. Raibert and J. J. Craig, "Hybrid position and force control of robot manipulators," *ASMS J. Dyna. Syst., Measure., Control*, vol. 102, pp. 126–133, June 1981.

[2] R. Anderson and M. W. Spong, "Hybrid impedance control of robotic manipulators," in *Proc. IEEE Int. Conf. Robotics Automation*, 1987, pp. 1073–1080.

[3] O. Khatib, "A unified approach for motion and force control of robot manipulators: The operational space formulation," *IEEE J. Robot. Automat.*, vol. RA-3, pp. 43–53, Jan. 1987.

[4] G. J. Liu and A. A. Goldenberg, "Robust hybrid impedance control of robot manipulators," in *Proc. IEEE Conf. Robotics Automation*, 1991, pp. 287–292.

[5] N. Hogan, "Impedance control: An approach to manipulator," *ASME J. Dyna. Syst., Measure., Control*, vol. 107, pp. 1–24, Mar. 1985.

[6] ——, "Stable execution of contact tasks using impedance control," in *Proc. IEEE Int. Conf. Robotics Automation*, 1987, pp. 1047–1054.

[7] E. Colgate and N. Hogan, "An analysis of contact instability in terms of passive physical equivalents," in *Proc. IEEE Int. Conf. Robotics Automation*, 1989, pp. 404–409.

[8] Y. S. Xu and R. P. Paul, "On position compensation and force control stability of a robot with a compliant wrist," in *Proc. 19th IEEE Conf. Robotics Automation*, 1988, pp. 1173–1178.

[9] A. A. Goldenberg, "Analysis of force control based on linear models," in *Proc. IEEE Conf. Robotics Automation*, 1992, pp. 1348–1353.

[10] T. Lasky and T. C. Hsia, "On force-tracking impedance control of robot manipulators," in *Proc. IEEE Int. Conf. Robotics Automation*, 1991, pp. 274–280.

[11] S. Lee and H. S. Lee, "Intelligent control of manipulators interfacing with an uncertain environment based on generalized impedance," in *Proc. IEEE Symp. Intelligent Control*, 1991, pp. 61–66.

[12] H. Seraji and R. Colbaugh, "Force tracking in impedance control," in *Proc. IEEE Int. Conf. Robotics Automation*, 1993.

[13] H. Seraji, "Adaptive admittance control: An approach to explicit force control in compliant motion," in *Proc. IEEE Int. Conf. Robotics Automation*, 1994, pp. 2705–2712.

[14] R. Colbaugh and A. Engelmann, "Adaptive compliant motion of manipulators: Theory and experiments," in *Proc. IEEE Int. Conf. Robotics Automation*, 1994, pp. 2719–2726.

[15] S. Jung, T. C. Hsia, and R. G. Bonitz, "On force tracking impedance control with unknown environment stiffness," in *Proc. IASTED Int. Conf. Robotics Manufacturing*, June 1995, pp. 181–184.

[16] S. Jung and T. C. Hsia, "Neural network techniques for robust force control of robot manipulators," in *Proc. IEEE Symp. Intelligent Control*, Monterey, CA, Aug. 1995, pp. 111–116.

[17] ——, "Neural network impedance force control of robot manipulators," *IEEE Trans. Ind. Electron.*, vol. 45, pp. 451–461, June 1998.

[18] ——, "Robust neural force control scheme under uncertainties in robot dynamics and unknown environment," *IEEE Trans. Ind. Electron.*, vol. 47, pp. 403–412, Apr. 2000.

[19] S. Jung, S. B. Yim, and T. C. Hsia, "Experimental studies of neural network impedance force control for robot manipulators," in *Proc. IEEE Conf. Robotics Automation*, May 2001, pp. 3453–3458.

[20] J. M. Tao and J. Y. S. Luh, "Application of neural network with real-time training to robust position/force control of multiple robots," in *Proc. IEEE Int. Conf. Robotics Automation*, 1993, pp. 142–148.

[21] K. Kiguchi and T. Fukuda, "Position/force control of robot manipulators for geometrically unknown objects using fuzzy neural networks," *IEEE Trans. Ind. Electron.*, vol. 47, pp. 641–649, June 2000.

[22] S. Jung and T. C. Hsia, "Adaptive force tracking impedance control of robot for cutting nonhomogeneous workpiece," in *Proc. IEEE Conf. Robotics Automation*, May 1999, pp. 1800–1804.

[23] T. C. Hsia, "Simple robust schemes for cartesian space control of robot manipulators," *Int. J. Robot. Automat.*, vol. 9, no. 4, pp. 167–174, 1994.

[24] ——, "Decoupled robust joint control of robot manipulators," in *Proc. 2nd IEEE Workshop Advanced Motion Control*, Nagoya, Japan, 1992, pp. 1–8.

[25] B. W. Drake and T. C. Hsia, "Implementation of a unified robot kinematics and inverse dynamics algorithm on a DSP chip," *IEEE Trans. Ind. Electron.*, vol. 40, pp. 190–195, Feb. 1993.

[26] R. G. Bonitz and T. C. Hsia, "Robust internal-force based impedance control for coordinating manipulators—Theory and experiments," in *Proc. IEEE Int. Conf. Robotics Automation*, 1996, pp. 622–628.